Surface melting of gallium single crystals

R. Trittibach, Ch. Grütter, and J. H. Bilgram
Laboratorium für Festkörperphysik, Eidgenössische Technische Hochschule, CH-8093 Zürich, Switzerland
(Received 8 November 1993; revised manuscript received 25 April 1994)

Optical properties of the Ga(010), Ga(111), and Ga(112) surfaces have been studied. Single crystals have been grown at UHV conditions and *in situ* ellipsometric techniques have been applied. On the Ga(112) surface the formation of a quasiliquid layer has been detected at temperatures below the bulk melting point T_m. The optical properties of the layer are close to the ones of the crystal bulk. The thickness of the quasiliquid layer increases with increasing temperature T. The functional character of the growth law of the quasiliquid layer of the Ga(112) surface is in agreement with the prediction of mean-field theory. In the temperature range $0.5 < T_m - T < 3.5$ K the increase in layer thickness can be described by a logarithmic growth law with a correlation length $\xi = 0.8 \pm 0.2$ nm. For temperatures $0 < T_m - T < 0.2$ K the increase in layer thickness can be described by a power-law growth with a Hamaker constant $W = (4.8 \pm 2.0) \times 10^{-18}$ mJ. There is a crossover from a logarithmic to a power-law growth of the layer in the temperature range $0.2 < T_m - T < 0.5$ K. The crossover thickness is comparable with the correlation length within the disordered or quasiliquid layer: $l_c^* = 0.7 \pm 0.1$ nm. Ga(010) and Ga(111) surfaces are stable against thermal disordering up to T_m. The highest stability has been observed at the Ga(010) surface. On the Ga(111) surface, changes in the refractive index have been detected while cycling the temperature up to the bulk melting temperature, whereas the extinction coefficient remains constant. Close to the melting point no drastical changes in n or k have been observed indicating that no enhanced disordering takes place close to T_m.

I. INTRODUCTION

Although melting is one of the most commonly observed order-disorder phase transitions, a microscopic theory of melting does not exist. Phenomenological thermodynamics cannot give insight into microscopic mechanisms involved in the melting of solids, but information on microscopic changes which mark the beginning of the transition may be instrumental in the development of microscopic models. Melting can be characterized by the change of physical properties. Typical properties which are affected by melting are the long-range order and the sheer modulus in the crystalline state. Some substances show drastic changes of the electronic properties upon melting. Well-known examples are semiconductors Si or Ge, which are metallic in the liquid state.

In this paper, we report on an experimental study of properties of surfaces of α-Ga single crystals at conditions close to the melting point by means of ellipsometric techniques. Ga has several advantages for such a study.

(1) The melting point temperature T_m(0 bar) = 29.7666 °C (Ref. 1) is close to room temperature.

(2) The vapor pressure of Ga at T_m is about 10^{-39} Pa.[2] Thus evaporation of the sample at T_m can be neglected and equilibrium conditions can be established easily.

(3) Ga is available at high purity.

(4) Ga single crystals can be grown easily.

(5) In the solid state two Ga atoms form covalently bound Ga_2 molecules, whereas liquid Ga is metallic.

(6) Ga crystals are highly anisotropic. Therefore, theories for surface melting can be tested experimentally for surfaces with various properties.

The properties of α-Ga and the α-Ga surfaces studied in our experiments are discussed in Sec. II. In Secs. III and IV, we present our experimental techniques and results. In Sec. V we discuss our data in the framework of a consideration of minimum free energy of the surface layer.

The structure of the crystal surface at temperatures just below the bulk melting point is of special interest in connection with the basic problem of describing the melting transition.[3,4] Atoms in the topmost surface layer are missing part of their nearest neighbors which gives rise to a charge redistribution in the near-surface region.[5] Long-range order is destroyed at the crystal surface during surface melting. A thin film with a liquidlike short-range order is formed at temperatures below T_m. As long as the disordered surface layer extends over a few monolayers only, the atoms in the disordered surface region are influenced by the presence of the ordered solid below. Such a premelted film is usually referred to as a *"quasiliquid layer,"* having properties assumed to be intermediate between those of the solid and the liquid. This quasiliquid layer is in thermal equilibrium with the underlying solid and its thickness depends on the temperature T of the sample only. As T approaches the bulk melting temperature T_m the layer thickness increases continuously. Infinitesimally close to T_m the melt front has penetrated deeply into the crystal, resulting in a coexistence of bulk solid, liquid, and vapor phases. Surface melting depends on the crystallographic orientations of the surfaces. The occurrence of a quasiliquid layer below the bulk melting temperature on the major part of a crys-

tal is invoked to explain the absence of superheating for the majority of solid materials: the formation of a liquid surface layer eliminates the need for liquid nucleation and thus no metastability effects exist.

Surface melting has proven hard to tackle by a conventional microscopic theory. A detailed treatment can be found in (Refs. 6 and 7). According to mean-field theory the free energy of the surface layer G_S per unit area is described by

$$G_S(l)=\gamma_{sl}+\gamma_{lv}+L_m(1-T/T_m)l+\Delta\gamma e^{-2l/\xi}+Wl^{-2}\ , \tag{1.1}$$

with l as the thickness of the layer and ξ the correlation length of the order parameter perpendicular to the surface. The first and the second terms in (1.1) represent the solid liquid, γ_{sl}, and the liquid vapor, γ_{lv}, interface free energies. The third term represents the free-energy cost associated with supercooling the melt liquid; L_m is the latent heat of melting per unit volume. This contribution to the free energy per unit area increases linearly with l. It leads to an effective attractive force per unit area between the solid-liquid and the liquid-vapor interfaces, which is equal to $L_m(1-T/T_m)$. Considering the fourth term, $\Delta\gamma$ is the free energy which the ordered solid-vapor interface has in excess of a surface which is completely wetted by the liquid phase:

$$\Delta\gamma:=\gamma_{sv}-(\gamma_{sl}+\gamma_{lv})\ . \tag{1.2}$$

$\Delta\gamma e^{-2l/\xi}$ represents the effective interaction energy between the solid-quasiliquid and the quasiliquid-vapor interfaces. This short-range contribution to $G_S(l)$ is related directly to short-range particle interactions and leads to an exponentially decaying force between the two interfaces. Wl^{-2} represents the interaction energy between the two interfaces due to van der Waals forces. This term decreases with l^{-2} with increasing layer thickness and is therefore called a long-range contribution to $G_S(l)$. Positive W favors the intercalation of a thick quasiliquid layer in between solid and liquid.

Regarding expression (1.1) four possible situations may be discussed, depending on attractive or repulsive long- and short-range forces. For the case $\Delta\gamma>0$ and $W>0$ the short-range contribution to $G_S(l)$ leads to an effective force between the solid-quasiliquid and the quasiliquid-vapor interface which is repulsive and favors large values of l. For $W>0$ the long-range contribution leads to a repulsive force as well. Minimizing $G_S(l)$ with respect to l yields the equilibrium thickness $l=l^*$. The crossover thickness l_c is defined as the thickness for which the long-range contribution to $dG_S(l)/dl$ is equal to the short-range contribution.[6] For $l^*\ll l_c$ the long-range contribution can be neglected and the equilibrium thickness is given by

$$l^*=\frac{\xi}{2}\ln\left[\frac{2\Delta\gamma T_m}{(T_m-T)L_m\xi}\right]\ . \tag{1.3}$$

For larger thickness $l^*\gg l_c$ the short-range contribution becomes negligible and the equilibrium thickness is then given by

$$l^*=\left[\frac{2WT_m}{(T_m-T)L_m}\right]^{1/3}\ . \tag{1.4}$$

Retardation effects in the fluctuating dipole interactions ultimately cause the exponent of the power law to change from $-1/3$ to $-1/4$, as T_m is approached.[6]

II. PROPERTIES OF GALLIUM

The optical properties of Ga change in two ways upon melting. (i) Ga forms in the crystalline α-state covalently bound Ga_2-molecules, whereas in the liquid state Ga is a monoatomic liquid metal.[8] Thus the electronic properties change upon melting. (ii) α-Ga is highly anisotropic. This anisotropy vanishes upon melting.

The crystal structure of α-Ga is orthorhombic with eight atoms per unit cell. The lattice constants a and c are almost identical ($a=0.4519$ nm, $c=0.4526$ nm) whereas the lattice constant b is approximately $\sqrt{3}a$ ($b=0.7657$ nm).[9] In literature at least three different versions can be found how to assign a,b,c to the three crystallographic axes. In this paper, the convention of Ref. 10 is used, which relates α-Ga to the space group Cmca. The orthorhombic structure is characterized by only one nearest-neighbor atom at 0.2442 nm and six next-nearest atoms, two at a distance of 0.2711, 0.2742, and 0.2801 nm, respectively.[9]

Single crystals of α-Ga grow in a characteristic shape (Fig. 1) from the melt. Four types of low-index facets are observed: (100), (010), (111), and (112). The (010) and (111) orientations form large facets which cover most of the surface of the single crystals; the (100) and (112) facets however are much smaller. Surfaces with large surface free energies and low packing densities are expected to decrease their free energy by a surface reconstruction or by surface melting upon heating close to T_m. The (112) facet is the one with lowest packing density of 2.5 dimers per nm^2, thus it might be a candidate to exhibit surface melting. The (100), (111), and (010) surfaces have dimer densities of 5.8, 7.5, and 9.8 dimers per nm^2, respectively.

Up to now optical properties of α-Ga have not been in-

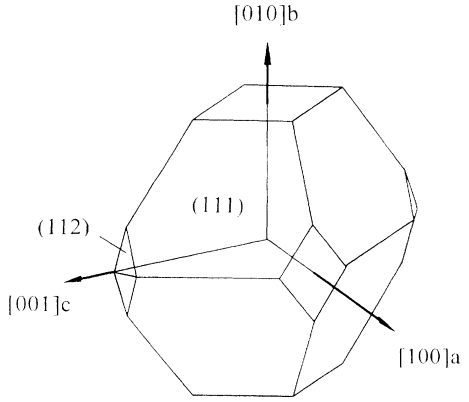

FIG. 1. Characteristic habitus of α-Ga single crystals grown from the melt. The surface orientations are labeled with the notation used in Ref. 10.

vestigated in great detail. The few existing values of the optical characteristics reported so far differ due to sample preparation (thin Ga films, α-Ga single crystals) and surface treatment (polishing, chemical treatment of the surfaces). Rapp, Shklyarevskii, and Yarovaya,[11] Bor and Bartholomew,[12] and Eichis and Skornyakov[13] have investigated the optical properties of thin polycrystalline Ga films in the visible and near ir and uv. α-Ga is anisotropic and its optical properties must be defined by three pairs of real constants (refractive index n, extinction coefficient k), one for each axis of the orthorhombic system to which it belongs. Lenham,[14,15] Rapp, Yarovaya, and Bondarenko,[16] and Kofman, Cheyssac, and Richard[17] have tried to determine the values of the optical constants along each axis. Lenham used polished single crystals grown from the supercooled melt, while Rapp, Yarovaya, and Bondarenko avoided the drawback due to polishing by growing single crystals from molten Ga poured onto a carefully cleaned flat glass introducing an oriented seed. Neither Lenham nor Rapp, Yarovaya, and Bondarenko protected the single-crystal surfaces from oxidation; the crystal surfaces were analyzed in atmosphere. In both studies the same experimental technique has been used: the sample was fixed with one of the crystal axes in the reflecting surface normal to the plane of incidence; the other two axes laid in this plane, one being fixed parallel to the surface normal.

Teshev and Shebzukhov[18] investigated the optical properties of liquid Ga under unspecified vacuum conditions by ellipsometric measurements at angles of incidence of 71° in the 400–1000-nm wavelength region. Measurements in this region have shown that with increasing temperature the refractive index n increases, while the extinction coefficient k decreases. In the visible region the changes in n and k are not large, in the infrared region they are more pronounced. As a whole the temperature dependence of k is greater than the one of n.

The first optical investigation of the solid-liquid transition in Ga was made by Kofman, Cheyssac, and Garrigos.[19] Reflectance of thin Ga films in the spectral range 300–900 nm was measured under clean primary vacuum for several temperatures around the melting point ($T=0$, 25, 29, 40, and 50 °C). When melting occurs, the reflectance increases considerably in the whole spectral range (about 20% at 600 nm).

III. EXPERIMENT

Surface phenomena have to be investigated with surface sensitive experimental methods. We use ellipsometry to characterize surfaces of Ga single crystals. Ellipsometry is able to characterize thin layers down to a coverage of less than one monolayer as well as thick films; the upper limit of film thickness to be studied is given by the penetration depth of the laserlight used. Considering a liquid Ga film covering a Ga crystal a film thickness up to about 10 nm can be characterized.

An ellipsometer uses polarized light to investigate the surface of a bulk solid or liquid, or thin films on top of a substrate, thus providing a noncontact and nondestructive investigation method. In ellipsometric measurements the surface of a sample is illuminated with monochromatic light of known wavelength and polarization and then the polarization of the reflected light is analyzed. Two ellipsometric angles Ψ and Δ are measured in the form

$$\rho = r_{pp}/r_{ss} = \tan\Psi e^{i\Delta} , \tag{3.1}$$

representing the ratio of the complex amplitude reflection coefficients for polarizations parallel (r_{pp}) and perpendicular (r_{ss}) to the plane of incidence. Ψ and Δ can be related to the index of refraction n and the extinction coefficient k of the investigated system. The thickness of a thin film can be determined, if the optical properties of the film and the underlying substrate are known. A detailed treatment of the various aspects of ellipsometry can be found in (Refs. 20–24).

To investigate surface disordering phenomena contamination free crystal surfaces are needed. The unusual low melting temperature of Ga does now allow to prepare clean surfaces by heating Ga single crystals. Therefore, we try to prevent contaminations in the bulk as well as at the surfaces by growing the crystals in a growth chamber at UHV conditions. The base pressure is in the 10^{-9} mbar range for the growth and the preparation chamber and in the 10^{-10} mbar range for the optical analysis chamber. For our experiments we use growth facets of crystals grown by means of the Nacken-Kyropoulos-technique.[25] The crystals are grown with a quasiconstant growth velocity of about 0.1 μm/s typically in a time of 20–30 h and have a size of about $1\times1\times1$ cm^3.

Thermal equilibrium between sample surface and bulk is a prerequisite for any reliable investigation of temperature-dependent surface structure. This demand is achieved by a homogeneous temperature within the experimental setup for a long period (days). Therefore, we have built a thermally insulated box around the whole optical analysis chamber. The measured temperature drift of the sample inside the optical analysis chamber is less than 5 mK per hour.

IV. MEASUREMENTS

In this section we present the results of ellipsometric measurements. We have adjusted the ellipsometer at UHV conditions using an alignment prism that can be inserted in the optical path of the laser beam. Adjustments are verified by test measurements using a silicon waver with known optical properties. We perform our measurements at an angle of incidence $\theta_i = 70°$. The surface of the Ga single crystal under study is adjusted by autocollimation of a HeNe-laser beam directed normal to the sample surface. We use the following notation: Data obtained at a crystal surface Ga(hkl) are labeled by an index (hkl). In the measurements the line of intersection of the crystal surface and the plane of incidence (defined by the propagation vector of the incident laser beam and the normal to the crystal surface) is oriented along the direction [xyz], e.g., Ψ measured on the Ga(010) surface with the line of intersection along the [100] direction will be denoted as $\Psi_{(010)}([100])$, and in the following desig-

nated as Ψ measured on the Ga(010) surface along the [100] direction.

In the first paragraph (Sec. IV A), we present the optical constants determined along the directions of the principal axes of the bulk crystal. In the second paragraph (Sec. IV B) the temperature dependence of the surface properties is studied at temperatures close to the melting temperature $T_m = 29.7666\,^{\circ}\mathrm{C}$ at 0 bar, which is identical with the triple point temperature.

A. Optical constants at room temperature

We have determined the refractive indices n and the extinction coefficients k along the three principal crystal axes a, b, and c of α-Ga single crystals at room temperature (25 °C). For the analysis of the ellipsometric measurements at the Ga(100) and the Ga(010) surface we used the method for orthorhombic crystals given by Graves.[24] Measurements along the [100] direction (a axis) and the [001] direction (c axis) have been performed on the Ga(010) surface, measurements along the [010] direction (b axis) on the Ga(100) surface.

Ellipsometric angles ($\lambda = 632.8$ nm): $\Psi_{(010)}([100]) = 35.3 \pm 0.1$, $\Psi_{(100)}([010]) = 30.3 \pm 0.1$, $\Psi_{(010)}([001]) = 32.4 \pm 0.1$, $\Delta_{(010)}([100]) = 134.6 \pm 0.5$, $\Delta_{(100)}([010]) = 152.1 \pm 0.5$, $\Delta_{(010)}([001]) = 154.8 \pm 0.5$. Refractive index ($\lambda = 632.8$ nm): $n([100]) = 2.9 \pm 0.3$, $n([010]) = 5.2 \pm 0.5$, $n([001]) = 6.0 \pm 0.7$. Extinction coefficient ($\lambda = 632.8$ nm): $k([100]) = 5.1 \pm 0.1$, $k([010]) = 4.7 \pm 0.1$, $k([001]) = 5.4 \pm 0.1$. Our measurements are in good agreement with the results of Rapp, Yarovaya, and Bondarenko[16] but differ from the values determined by Kofman, Cheyssac, and Richard.[17]

B. Temperature dependence of surface properties

We have investigated the low-index Ga(010), Ga(111), and Ga(112) surfaces close to the melting point. These surfaces are naturally existing facets on bulk crystals grown from the melt.

Ellipsometric angles Ψ and Δ have been measured in the temperature range $T_0 < T < T_m$, where T_0 is the temperature where measurements have been started. Temperature has been increased by typically 50 mK per hour up to T_m. In the range $0 < T_m - T < 100$ mK the increase in temperature has been reduced to typically 10 mK per hour. Cycling the temperature several times from the starting temperature T_0 to a temperature close to T_m leads to reproducible data for Ψ and Δ. No hysteresis effects have been detected, indicating that the sample has been very close to thermal equilibrium during measurements. We have used the model of an optically isotropic substrate to determine the refractive index n and the extinction coefficient k for the measurements on different crystal faces along different directions.

Ga(010) surface. Measurements have been performed along the [100] direction for temperatures in the range $0 < T_m - T < 2$ K. The variations in the refractive index and the extinction coefficient are about 0.4% and 0.1% of the values $n_{(010)}([100]) = 2.44$ and $k_{(010)}([100]) = 5.04$, respectively, at the starting temperature T_0, $T_m - T_0 = 2$ K. These results indicate that the (010) surface is stable up to the melting temperature.

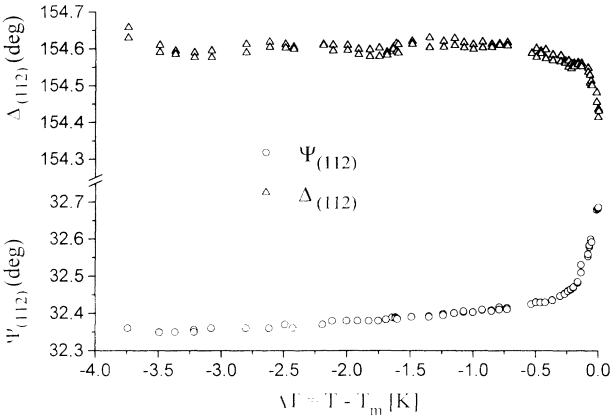

FIG. 2. Experimental data Ψ and Δ as measured at temperatures close to T_m at the Ga(112) surface along the $[\bar{1}\,\bar{1}1]$ direction. It is found that data deviate from the room temperature data if $T_m - T < 2$ K. The error bars are small compared to the symbols used in the plot.

Ga(111) surface. Measurements have been performed along the $[\bar{1}10]$ direction for temperatures in the range $0 < T_m - T < 4.5$ K. The variations in the refractive index and extinction coefficient are about 0.4% and 0.1% of the values $n_{(111)}([\bar{1}10]) = 4.40$ and $k_{(111)}([\bar{1}10]) = 4.79$, respectively, at the starting temperature T_0, $T_m - T_0 = 4.5$ K. Changes in the refractive index $n_{(111)}([\bar{1}10])$ are bigger than the corresponding changes observed at the Ga(010) surface, but no systematic variations with increasing temperature have been found.

Ga(112) surface. Measurements have been performed along the $[\bar{1}\,\bar{1}1]$ direction for temperatures in the range $0 < T_m - T < 3.5$ K. Δ and Ψ as measured are plotted in Fig. 2 as a function of temperature.

V. DISCUSSION

Stability of the Ga(010) surface. For temperatures with $0 < T_m - T < 2$ K no changes for n and k have been found. From that we conclude that no surface induced premelting or disordering phenomena can be identified in the experiments. The surface seems to be stable up to the bulk melting temperature T_m. The stability of the Ga(010) surface close to the melting point deduced from the ellipsometric measurements can be explained by the (1×1)-reconstruction of the surface detected in a STM study.[26]

Stability of the Ga(111) surface. Only small changes in the refractive index have been detected while increasing the temperature up to the bulk melting temperature, whereas the extinction coefficient remains constant. Close to the melting point no drastic changes in n or k have been observed. The Ga(111) surface seems to be stable up to the bulk melting temperature. Ellipsometric measurements are in agreement with scanning-tunneling-microscopy (STM) studies[26] of this surface where thermally initiated disordering has not been observed, but an increase in tip-induced surface

modifications with increasing temperature during measurements gives rise to the assumption of a temperature dependent ductility of the topmost surface layers. No surface reconstruction has been detected at the Ga(111) surface by means of STM.[26] Thus, the surface free energy of the Ga(111) surface is assumed to be higher than the one of the Ga(010) surface.

Disordering of the Ga(112) surface. Assuming that surface melting takes place at the Ga(112) surface the behavior of the ellipsometric angles $\Psi_{(112)}([\bar{1}\,\bar{1}1])$ and $\Delta_{(112)}([\bar{1}\,\bar{1}1])$ show that a disordered layer is growing with increasing temperature. In the following we show how the experimentally measured variations in the ellipsometric angles, $\delta\Psi_{(112)}[(\bar{1}\,\bar{1}1])$ and $\delta\Delta_{(112)}([\bar{1}\,\bar{1}1])$, can be related to the thickness and the optical properties of the growing layer. Performing model calculations we determine in a first step the optical constants and the thickness of the layer. Then we use these data to evaluate which of the models of surface melting are applicable to our system and determine the correlation length in the layer and the Hamaker constant.

We use the simple model of an isotropic substrate with optical properties determined at the starting temperature, $T_m - T = 3.5$ K, covering by a homogeneous, isotropic layer and calculate $\delta\Psi$ and $\delta\Delta$ as a function of the increasing layer thickness for various optical constants (refractive index n and extinction coefficient k) of the layer. To compare the computed values, $\delta\Psi$ and $\delta\Delta$, with the experimental data, we plot $\delta\Delta$ vs $\delta\Psi$ with the layer thickness l^* as the variable parameter. l^* increases along the curve. As shown in Fig. 3 the measured data, $\delta\Delta_{(112)}([\bar{1}\,\bar{1}1])$ vs $\delta\Psi_{(112)}([\bar{1}\,\bar{1}1])$, are compatible with the assumption of the formation of a layer with refractive index $n = 5.80 \pm 0.10$ and extinction coefficient $k = 5.65 \pm 0.05$. Thus, the optical properties of the layer are close to the ones of the crystal bulk. We have included in Fig. 3 a model calculation assuming that the layer has the properties of the liquid. The optical constants of the bulk liquid are $n = 1.50$ and $k = 7.25$ as determined

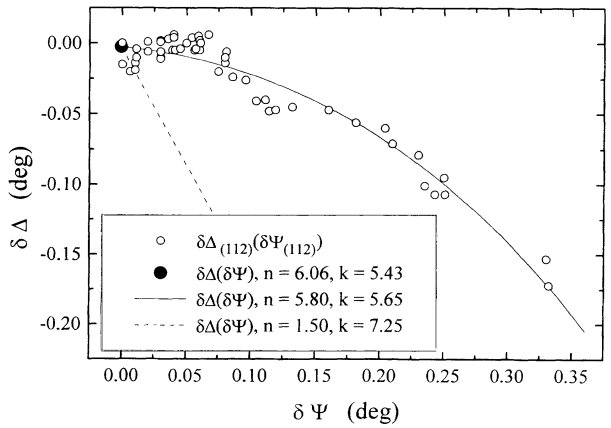

FIG. 3. Experimental data $\delta\Delta_{(112)}([\bar{1}\,\bar{1}1])$ are plotted vs $\delta\Psi_{(112)}([\bar{1}\,\bar{1}1])$ (open circles). The line drawn through the data points corresponds to a model calculation for a layer with a refractive index $n = 5.80$ and an extinction coefficient $k = 5.65$. The parameter increasing along the line is the thickness of the quasiliquid layer δl^* with $\delta l^* = 0$ nm at $\delta\Psi = 0, \delta\Delta = 0$ up to $\delta l^* = 3.75$ nm at $\delta\Psi = 0.33$, $\delta\Delta = -0.17$. The closed circle represents the crystal bulk with $n = 6.06$, $k = 5.43$. A layer with the properties of the bulk liquid, $n = 1.50$, $k = 7.25$, according to Ref. 18, is indicated by a dashed line. The parameter increasing along the drawn line is the thickness of the liquid layer starting with $\delta l^* = 0$ nm at $\delta\Psi = 0$, $\delta\Delta = 0$ up to $\delta l^* = 0.11$ nm at $\delta\Psi = 0.13$, $\delta\Delta = -0.22$. This diagram shows that the experimental data obtained at the (112) surface can be interpreted by the growth of a quasiliquid layer with optical properties close the ones of the bulk crystal.

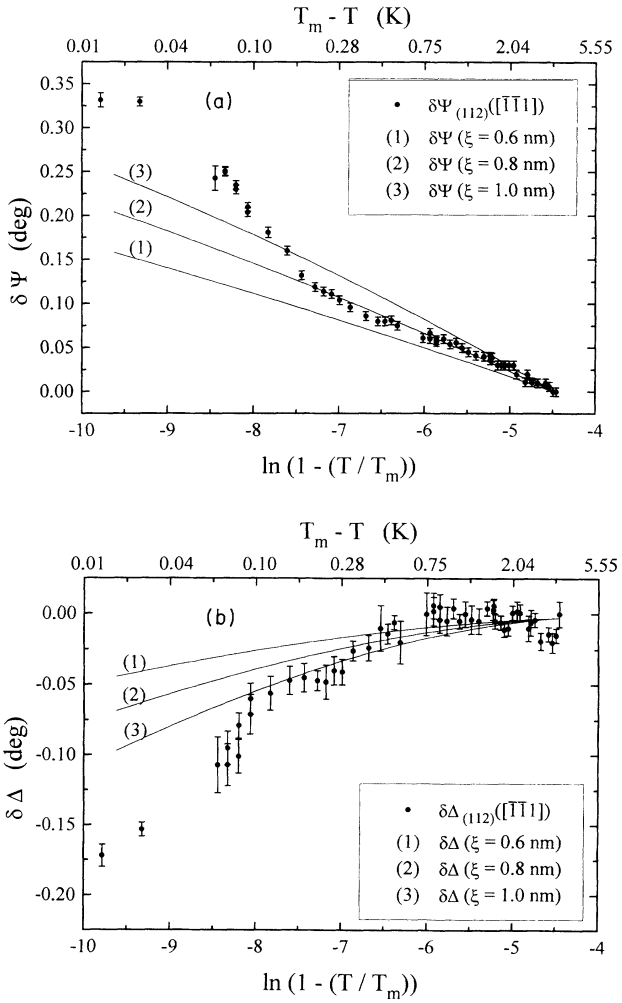

FIG. 4. (a) Experimental data $\delta\Psi_{(112)}([\bar{1}\,\bar{1}1])$ are plotted vs $\ln[1-(T/T_m)]$. These data are compared with model calculations of $\delta\Psi(\delta l^*)$ using the optical properties of the layer ($n = 5.80$ $k = 5.65$) and Eq. (1.3) assuming logarithmic growth of the layer with increasing temperature. The curve parameter is the correlation length ξ in the layer. (b) Experimental data $\delta\Delta_{(112)}([\bar{1}\,\bar{1}1])$ are plotted vs $\ln[1-(T/T_m)]$. These data are compared with model calculations of $\delta\Delta(\delta l^*)$ using the optical properties of the layer ($n = 5.80, k = 5.65$) and Eq. (1.3) assuming logarithmic growth of the layer with increasing temperature. The curve parameter is the correlation length ξ in the layer. Best agreement between experimental data and model calculations is obtained in the temperature range $0.5 < T_m - T < 3.5$ K, $\{-6.4 < \ln[1-(T/T_m)] < -4.5\}$, for a correlation length $\xi = (0.8 \pm 0.2)$ nm in the growing layer.

by extrapolation of the values of Teshev and Shebzukhov[18] to the melting temperature for a wavelength $\lambda=632.8$ nm. The comparison of these two data sets shows that the model calculations are very sensitive to the optical constants used. The variation of $\delta\Delta_{(112)}(\delta\Psi_{(112)})$ corresponds to an increase in the layer thickness, δl^*, of about 3.75 nm.

Using these data it is possible to determine the temperature dependence of the layer thickness. Once more we perform model calculations. Now we compare the measured, temperature-dependent variation in ellipsometric angles, $\delta\Psi_{(112)}([\bar{1}\,\bar{1}1])$ and $\delta\Delta_{(112)}([\bar{1}\,\bar{1}1])$, with a family of curves $\delta\Delta(l^*)$ and $\delta\Psi(l^*)$. We study two models: (i) a logarithmic growth of the layer ($n=5.80, k=5.65$) with increasing temperature, according to Eq. (1.3), computed for different values of the correlation length ξ of the layer [see Figs. 4(a), 4(b)]; (ii) a power law growth of the layer ($n=5.80, k=5.65$) with increasing temperature, according to Eq. (1.4), calculated for various values of the Hamaker constant W of the (112) surface [see Figs. 5(a), 5(b)].

In the temperature range $0.5<T_m-T<3.5$ K, $\{-6.4<\ln[1-(T/T_m)]<-4.5\}$, the increase in layer thickness can be described by a logarithmic growth with a correlation length $\xi=(0.8\pm0.2)$ nm, which is, as expected, longer than the correlation length within the liquid phase, $\xi_1=0.5$ nm. For temperatures $0<T_m-T<0.2$ K, $\{0<[1-(T/T_m)]^{1/3}<0.09\}$, the increase in layer thickness can be described by a power law growth with a Hamaker constant $W=(4.8\pm2.0)\times10^{-18}$ mJ.

We conclude that the increase in layer thickness l^* is determined by short-range forces at temperatures $T_m-T>0.5$ K, and by long-range forces at temperatures $T_m-T<0.2$ K. There is a crossover from a logarithmic to a power-law growth of the layer in the temperature range $0.2<T_m-T<0.5$ K (see Fig. 6). The thickness where crossover occurs is comparable with the correlation length within the disordered or quasiliquid layer: $l_c^*=(0.7\pm0.1)$ nm.

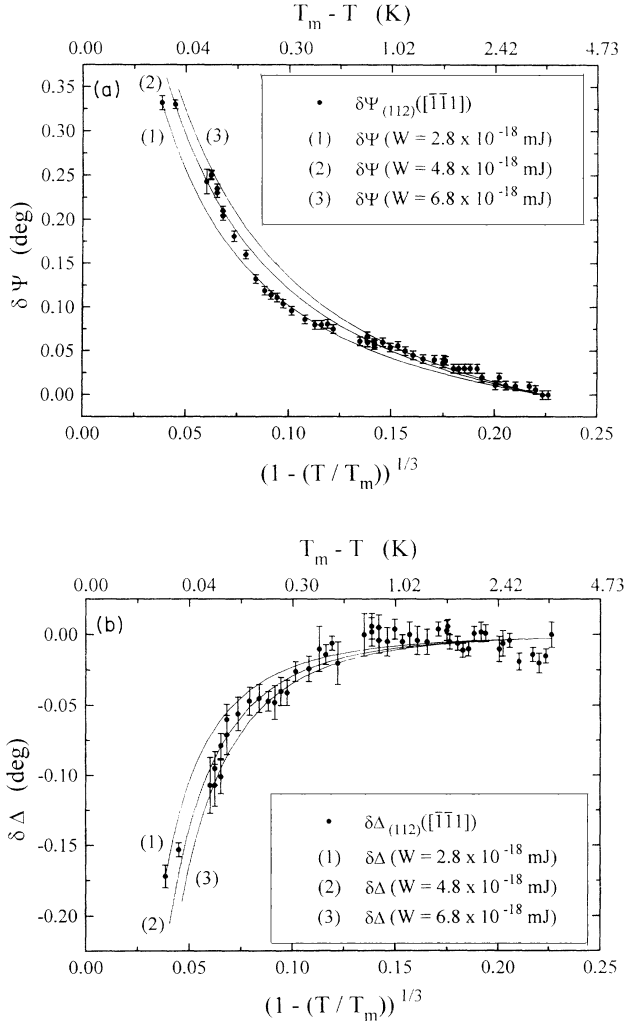

FIG. 5. (a) Experimental data $\delta\Psi_{(112)}([\bar{1}\,\bar{1}1])$ are plotted vs $[1-(T/T_m)]^{1/3}$. These data are compared with model calculations of $\delta\Psi(\delta l^*)$ using the optical properties of the layer ($n=5.80, k=5.65$) and Eq. (1.4) assuming a power-law growth of the layer with increasing temperature. The curve parameter is the Hamaker constant W. (b) Experimental data $\delta\Delta_{(112)}([\bar{1}\,\bar{1}1])$ are plotted vs $[1-(T/T_m)]^{1/3}$. These data are compared with model calculations of $\delta\Delta(\delta l^*)$ using the optical properties of the layer ($n=5.80, k=5.65$) and Eq. (1.4) assuming a power-law growth of the layer with increasing temperature. The curve parameter is the Hamaker constant W. Best agreement between experimental data and model calculations is obtained in the temperature range $0<T_m-T<0.2$ K, $\{0<[1-(T/T_m)]^{1/3}<0.09\}$, for $W=(4.8\pm2.0)\times10^{-18}$ mJ.

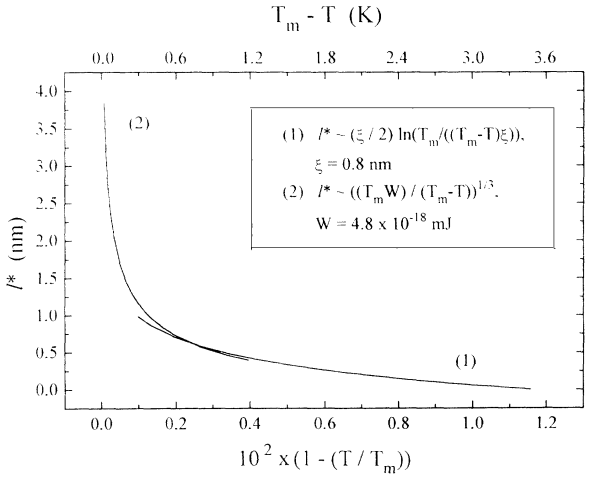

FIG. 6. Layer thickness l^* is plotted vs $1-T/T_m$. The increase in thickness is determined by a logarithmic growth for "low" temperatures $T_m-T>0.5$ K, $[(1-T/T_m)\times10^2>0.165]$, with a correlation length $\xi=0.8$ nm, and by a power-law growth for "high" temperatures $T_m-T<0.2$ K, $[(1-T/T_m)\times10^2<0.065]$, with a Hamaker constant $W=4.8\times10^{-18}$ mJ. A crossover from logarithmic to power-law growth takes place in the temperature range $0.5<T_m-T<0.2$ K $[0.165>(1-T/T_m)\times10^2>0.065]$. The crossover thickness is comparable with the correlation length in the layer: $l_c^*=(0.7\pm0.1)$ nm.

VI. CONCLUSION

We have investigated the Ga(010), Ga(111), and Ga(112) surfaces naturally existing on bulk crystals grown from the melt. The thermal behavior up to the bulk melting temperature T_m is determined by the atomic structure of these surfaces and can be discussed in terms of a simplified mean-field theory of surface melting based on the introduction of phenomenological surface free energies. Ga(010) and Ga(111) surfaces are stable against thermal disordering up to T_m whereas at Ga(112) surfaces the formation of a disordered or quasiliquid layer growing with increasing temperature has been observed.

Highest stability has been observed at the Ga(010) surface. This result is in agreement with a STM study.[26] The Ga(111) surface is not as stable as the Ga(010) surface. Changes in the refractive index have been detected while cycling the temperature up to the bulk melting temperature, whereas the extinction coefficient remains constant. Close to the melting point no drastic changes in n or in k have been observed indicating that no enhanced disordering occurs close to T_m. Ellipsometric measurements are in agreement with the results of a STM study[26] of this surface. In the STM study no thermally initiated disordering has been observed, but an increase of tip-induced surface modifications with increasing temperature during measurements give rise to the assumption of a temperature-dependent ductility of the topmost surface layers. No surface reconstruction has been detected at the Ga(111) surface by means of STM.[26] Thus, the surface free energy of the Ga(111) surface, $\gamma_{sv}(111)$, is assumed to be larger than the one of the Ga(010) surface.

The structure of the Ga(112) surface as deduced from the truncated crystal bulk is characterized by a low density of Ga_2 dimers. The surface free energy $\gamma_{sv}(112)$ is expected to be highest compared to other facets with different crystallographic orientations on bulk crystals grown from the melt. Referring to general predictions of surface melting, this surface should be a candidate to show a structural transition or thermally induced disordering close to the bulk melting temperature. Indeed, the formation of a layer has been detected. The optical properties of the layer are close to the ones of the crystal bulk. The thickness of the quasiliquid layer increases with increasing temperature.

In the temperature range $3.5 > T_m - T > 0.5$ K the increase in layer thickness can be described by a logarithmic growth with a correlation length $\xi = (0.8 \pm 0.2)$ nm. ξ exceeds the correlation length in the liquid phase ($\xi_1 = 0.5$ nm) as expected. For temperatures very close to T_m ($0.2 > T_m - T > 0$ K) the increase in layer thickness can be described by a power law growth with a Hamaker constant $W = (4.8 \pm 2.0) \times 10^{-18}$ mJ. The increase in layer thickness l^* is determined by short-range forces at temperatures $T_m - T > 0.5$ K, by long-range forces at temperatures $T_m - T < 0.2$ K. There is a crossover from a logarithmic to a power-law growth of the layer in the temperature range $0.2 < T_m - T < 0.5$ K. The crossover thickness is comparable with the correlation length within the disordered or quasiliquid layer: $l_c^* = (0.7 \pm 0.1)$ nm. Thus, in the case of the Ga(112) surface both the short-range as well as the long-range contributions to the surface free energy assist in the formation of a quasiliquid layer. The functional character of the growth law of the quasiliquid layer at the Ga(112) surface is in agreement with the prediction of mean-field theory. This experimental result is similar to results found at the Pb(110) surface.[6] The onset temperature for surface melting for Ga is much closer to T_m as in the case of Pb. The optical properties of the quasiliquid layer are different from the ones of the bulk liquid. This observation is complementary to diffraction experiments. Further experiments will be necessary to give detailed description of the nature of the quasiliquid layer at Ga.

ACKNOWLEDGMENTS

Our gratitude goes to our colleagues and collaborators. We would like to thank H. R. Aeschbach. His technical assistance in constructing and operating the mechanical equipment was very helpful. We also thank J. P. Stucki and M. Maier for their help with the design of parts of the UHV system, B. Nussberger for manufacturing the glass devices, and the internal mechanic staff for the construction of many mechanical parts of the experimental setup. We thank U. Dürig and O. Züger of the IBM Research Laboratory for the critical discussions concerning experimental and theoretical aspects of our work. We thank Professor Dr. H. R. Ott for support of our experiments. We also acknowledge J. Peisl. This work has been supported by the Swiss National Science Foundation.

[1] H. Preston-Thomas, Metrologia **27**, 3 (1990).
[2] T. Ilda and Roderick I. L. Gutherie, *The Physical Properties of Liquid Metals* (Clarendon Press, Oxford, 1988).
[3] J. G. Dash, Contemp. Phys. **30**, 89 (1989).
[4] E. Tosatti, in *The Structure of Surfaces II,* edited by J. F. van der Veen and M. A. Hove, Springer Series in Surface Sciences Vol. II (Springer, Berlin, 1987).
[5] K. Kern, in *Phase Transitions in Surface Films 2,* edited by H. Taub *et al.* (Plenum, New York, 1991).
[6] B. Pluis, D. Frenkel, and J. F. van der Veen, Surf. Sci. **239**, 282 (1990).
[7] R. Lipowsky, Ferroelectrics **73**, 69 (1987).
[8] A. Bizid, R. Cortes, A. Defrain, and C. Regnaut, J. Chim. Phys. **77**, 779 (1980).
[9] A. Defrain, J. Chim. Phys. **74**, 851 (1977).
[10] *International Tables for Crystallography* (Reidel, Dordrecht, 1983), Vol A.
[11] I. Yu. Rapp, I. N. Shklyarevskii, and R. G. Yarovaya, Fiz.

Tverd. Tela (Leningrad) **10**, 2257 (1968) [Sov. Phys. Solid State **10**, 1780 (1963)].
[12]J. Bor and C. Bartholomew, Proc. Phys. Soc. London **90**, 1153 (1967).
[13]A. Yu. Eichis and G. P. Skornyakov, Opt. Spectrosk. **16**, 159 (1964) [Opt. Spectrosc. (USSR) **16**, 86 (1964)].
[14]A. P. Lenham, Proc. Phys. Soc. London **82**, 933 (1963).
[15]A. P. Lenham and D. M. Treherne, J. Opt. Soc. Am. **56**, 752 (1966).
[16]I. Yu. Rapp, R. G. Yarovaya, and L. A. Bondarenko, Fiz. Tverd. Metalloved. **32**, 728 (1971) [Phys. Met. Metallogr. (USSR) **32**, 53 (1971)].
[17]R. Kofman, P. Cheyssac, and J. Richard, Phys. Rev. B **16**, 5216 (1977).
[18]R. Sh. Teshev and A. A. Shebzukhov, Opt. Spektrosk. **65**, 1178 (1988) [Opt. Spectrosc. (USSR) **65**, 693 (1988)].
[19]R. Kofman, P. Cheyssac, and R. Garrigos, J. Phys. F **9**, 2345 (1979).
[20]R. M. A. Azzam and N. M. Bashara, *Ellipsometry and Polarized Light* (North-Holland, Amsterdam, 1977).
[21]S. Teitler and B. Henvis, J. Opt. Soc. Am. **60**, 830 (1970).
[22]D. W. Berreman and T. J. Scheffer, Phys. Rev. Lett. **25**, 577 (1970).
[23]D. W. Berreman, J. Opt. Soc. Am. **62**, 502 (1972).
[24]R. H. W. Graves. J. Opt. Soc. Am. **59**, 1225 (1969).
[25]H. E. Buckley, *Crystal Growth* (Wiley, New York, 1951).
[26]O. Züger and U. Dürig, Phys. Rev. B **46**, 7319 (1992).